

**TRAILING-EDGE NOISE ATTENUATION OF AIRFOIL
BY MEANS OF COMB-SERRATION AT LOW
REYNOLDS NUMBERS**

BY

MOHAMED IBREN HASSAN

**A thesis submitted in fulfilment of the requirement for the
degree of Doctor of Philosophy in Engineering**

**Kulliyyah of Engineering
International Islamic University Malaysia**

NOVEMBER 2023

ABSTRACT

Low Reynolds number flow is three-dimensional and intricate due to multiple vortical phenomena. This research contributes by investigating the impact of laminar Separation Bubble (LSB) on noise generated by passive control techniques. It also enhances the understanding of the efficiency of various trailing edge designs such as serrations, comb, comb-serrated, and porous configurations, across different flow conditions and Reynolds numbers, while also addressing the limitations of existing geometrical models for trailing edges. The study intends to examine the performance of different configurations, emphasizing their effect on flow structure and acoustic responses. The methodology of this study encompasses a combination of techniques that includes conducting 2D simulations using the SST model, performing 3D simulations using large eddy simulation, employing FW-H acoustic modeling, and utilizing an experimental PIV setup. These methods collectively provide a comprehensive and robust platform for in-depth exploration of the research objectives. The analysis of the NACA0015 airfoil's flow characteristics revealed the presence of laminar separation bubbles (LSBs) at low Reynolds numbers and angles of attack. Two types of flow patterns, with and without reattachment, were identified. On the suction side, increasing the Angle of attack leads to a noticeable upstream shift of these points, while they move downstream along the pressure side. In 3D simulations, pressure distribution was symmetrical, with the maximum at the leading edge. No separation was observed except at the trailing edge tip. At higher angles of attack, the baseline airfoil experienced flow disturbances, laminar separation bubbles, and vortex shedding. The serrated, combed, and comb-serrated designs exhibited more stable flow patterns and fewer separation bubbles than the baseline, potentially reducing tonal noise. Conversely, the poro-serrated design led to distorted flow and an upstream-moving separation bubble, suggesting a possible increase in tonal noise. Moreover, results showed irregular broadband noise (300 - 600 Hz) with increased noise and shifting peak frequency as the Angle of attack rose. The serrated trailing edge design notably reduced noise levels by roughly 21 dB, especially for low frequencies. Comb-serration increased high-frequency noise by about 9 dB for angles of attack at 0, -1, and -2 degrees reduced approximately 9 dB for angles of attack at 1 degree and 2 degrees. On the other hand, the directivity pattern showed that the maximum noise level is observed to predominantly radiate at an azimuth angle of around 90 degrees for all the cases, ranging from 90 to 270 degrees, indicating that the majority of the source's acoustic energy is being emitted on the suction and pressure sides of the wing. In conclusion, the findings demonstrate that serrated and comb-serrated designs are beneficial in reducing noise levels, and that the Angle of attack can significantly impact both the noise level and directivity pattern.

خلاصة البحث

تدفق أرقام رينولدز المنخفض ثلاثي الأبعاد معقد للغاية بطبيعته لتعدد أنواع الظواهر الدوامية. يساهم هذا البحث من خلال دراسة تأثير فقاعة الفصل الصفائحي (LSB) على الضوضاء الناتجة عن تقنيات التحكم السليبي. كما يحسن فهم كفاءة تصميمات الحواف الخلفية المختلفة مثل المسننات، والمشط، والمشط المسنن، والتكوينات المسامية، عبر مختلف حالات التدفق وأرقام رينولدز، مع معالجة القصور في النماذج الهندسية الموجودة للحواف الخلفية. الدراسة تهدف إلى فحص أداء تكوينات مختلفة، مع التركيز على تأثيرها على بنية التدفق والاستجابات الصوتية. منهجية الدراسة تشمل مزيجاً من التقنيات، تتضمن إجراء عمليات محاكاة ثنائية الأبعاد باستخدام نموذج SST و عمليات محاكاة ثلاثية الأبعاد باستخدام LES، واستخدام نموذج صوتي FW-H وإعدادات PIV التجريبي. هذه الأساليب مجتمعة توفر منصة شاملة وقوية للاستكشاف المتعمق لأهداف البحث. كشف تحليل خصائص تدفق الجنيح NACA0015 عن وجود فقاعات الفصل الصفائحي (LSBs) عند أعداد رينولدز المنخفضة وزوايا الهجوم. تم تحديد نوعين من أنماط التدفق، مع وبدون إعادة الارتباط. من جهة الشفط، تؤدي زيادة زاوية الهجوم إلى تحول ملحوظ في الاتجاه الصعودي لهذه النقاط نحو المنبع، بينما تتحرك باتجاه نزولي على طول جانب الضغط. في عمليات المحاكاة ثلاثية الأبعاد، كان توزيع الضغط متماثلاً، مع حد أقصى عند الحافة الأمامية. لم يلاحظ أي انفصال إلا عند طرف الحافة الخلفية. عند زوايا الهجوم الأعلى، تعرض الجنيح الأساسي لاضطرابات التدفق، وفقاعات الفصل الصفائحي، وتساقط الدوامية. أظهرت التصميمات المسننة والمشطية والمسننة أنماط تدفق أكثر استقراراً وفقاعات فصل أقل مقارنة بالأساس، مما يؤدي إلى تقليل الضوضاء النغمية. على العكس من ذلك، أدى التصميم المسنن المسامي إلى تدفق مشوه وفقاعة فصل تتحرك في اتجاه صعودي، مما يشير إلى زيادة محتملة في الضوضاء النغمية. علاوة على ذلك، أظهرت النتائج عدم انتظام ضوضاء النطاق العريض (300 - 600 هرتز) مع زيادة الضوضاء وتغير تردد الذروة كلما ارتفعت زاوية الهجوم. أدى تصميم الحافة الخلفية المسننة إلى تقليل مستويات الضوضاء بشكل ملحوظ بحوالي 21 ديسيبل، خاصة بالنسبة للترددات المنخفضة. أدى المشط المسنن إلى زيادة الضوضاء عالية التردد بنحو 9 ديسيبل لزوايا الهجوم عند درجات 0 و-1 و-2، كما حقق انخفاضاً بنحو 9 ديسيبل لزوايا الهجوم عند درجة ودرجتين. من ناحية أخرى، أظهر نمط الاتجاه أن مستوى الضوضاء الأقصى يشع في الغالب بزواوية سمت تبلغ حوالي 90 درجة لجميع الحالات، وتتراوح من 90 إلى 270 درجة، مما يشير إلى أن غالبية مصدر الطاقة الصوتية للمصدر تنبعث على جانبي الشفط والضغط للجناح. في الختام، أظهرت النتائج أن التصميمات المسننة والمشطية مفيدة في تقليل مستويات الضوضاء، خاصة عند زوايا الهجوم العالية، وأن زاوية الهجوم يمكن أن يكون لها تأثير كبير على كل من مستوى الضوضاء ونمط الاتجاه.

APPROVAL PAGE

The thesis of Mohamed Ibren Hassan has been approved by the following:



Amelda Dianne Binti Andan
Supervisor



Waqar Asrar
Chairman/ Co-Supervisor

Moumen Mohammed Mahmoud Idres
Internal Examiner

Azmin Shakrine Mohd Rafie
External Examiner

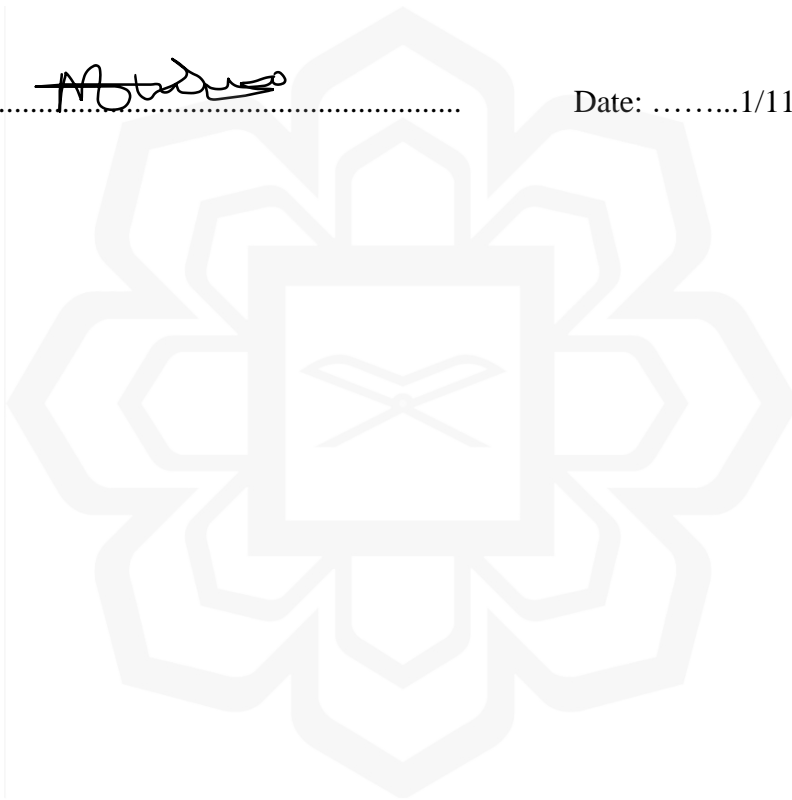
Akram M Z M Khedher
Chairman

DECLARATION

I hereby declare that this thesis is the result of my own investigations, except where otherwise stated. I also declare that it has not been previously or concurrently submitted as a whole for any other degrees at IIUM or other institutions.

Mohamed Ibren Hassan

Signature  Date:1/11/2023.....



**DECLARATION OF COPYRIGHT AND AFFIRMATION OF
FAIR USE OF UNPUBLISHED RESEARCH**

**TRAILING-EDGE NOISE ATTENUATION OF AIRFOIL BY
MEANS OF COMB-SERRATION AT LOW REYNOLDS
NUMBERS**

I declare that the copyright holders of this Thesis are jointly owned by the student and IIUM.

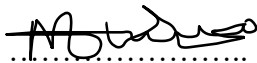
Copyright © 2023 Mohamed Ibren and International Islamic University Malaysia. All rights reserved.

No part of this unpublished research may be reproduced, stored in a retrieval system, or transmitted, in any form or by any means, electronic, mechanical, photocopying, recording or otherwise without prior written permission of the copyright holder except as provided below.

1. Any material contained in or derived from this unpublished research may be used by others in their writing with due acknowledgement.
2. IIUM or its library will have the right to make and transmit copies (print or electronic) for institutional and academic purposes.
3. The IIUM library will have the right to make, store in a retrieved system and supply copies of this unpublished research if requested by other universities and research libraries.

By signing this form, I acknowledged that I have read and understand the IIUM Intellectual Property Right and Commercialization policy.

Affirmed by Mohamed Ibren Hassan


.....

Signature

.....1/11/2023.....

Date

ACKNOWLEDGEMENTS

In the Name of Allah, the Most Compassionate, the Most Merciful

With the blessings of Allah, the Most Merciful, the Most Compassionate, I begin this acknowledgement. All glory and praise belongs to Allah, the Sovereign Lord of all creation, and, peace be upon our beloved Prophet Mohammed (peace be upon Him).

I would like to express my sincere gratitude and offer my heartfelt thanks to all those who have supported me in this endeavor. Their encouragement and unwavering support have been a source of inspiration for me and has enabled me to reach this point. I am truly grateful for their presence in my life and the role they have played in helping me achieve this milestone.

I would like to express my sincerest gratitude to the aerodynamics laboratory of Universiti Pertahanan Nasional Malaysia (UPNM) for their generous support and provision of essential equipment that has enabled me to carry out my experimental work. I am deeply thankful to my colleagues in our mechanical lab for their tremendous collaboration and encouragement throughout this journey. I would like to extend a special recognition to my supervisory committee consisting of Dr. Amelda Dianne Binti Andan, Professor Waqar Asrar, and Dr. Erwin Suleiman, for their unwavering encouragement, guidance, and support. Their invaluable advice, constructive feedback, and relentless dedication to my success have been an integral part of my journey. I would also like to extend my acknowledgement to Dr. Mohammed Abdulmalek Aldheeb for his invaluable input and assistance in my experimental work. I am truly grateful for the support and guidance I have received from everyone involved in this project. Their contributions have made this experience truly enriching and rewarding.

My sincerest thanks go to my parents and my wife for their unwavering belief in me and their immense patience throughout this study. Their support has been invaluable, and I am deeply grateful. I would also like to extend my gratitude to my siblings for their constant encouragement and prayers throughout my life. Their love and support have been a constant source of strength and motivation, and I am blessed to have them in my life.

TABLE OF CONTENTS

Abstract	ii
Abstract in Arabic	iii
Approval Page.....	iv
Declaration	v
Copyright Page.....	vi
Acknowledgements	vii
Table of Contents	viii
List of Tables	xi
List of Figures	xii
List of Symbols	xvi
List of Abbreviations	xvii
CHAPTER ONE: INTRODUCTION	1
1.1. Overview.....	1
1.2. Background of the Study	1
1.3. Statement of the Problem.....	4
1.4. Research Philosophy.....	6
1.5. Research Objectives.....	6
1.6. Research Scope	6
1.7. Limitations of the Study	8
1.8. Significance of the Study.....	8
1.9. Thesis Structure	9
CHAPTER TWO: LITERATURE REVIEW.....	10
2.1. Overview.....	10
2.2. Flow Structure at Low Reynold’s Number.....	10
2.3. Noise Mechanisms.....	14
2.3.1. Types of Noise	14
2.3.2. Noise Generation Mechanism.....	16
2.3.3. Factors Affecting Airfoil Noise	18
2.4. Flow and Noise Control.....	20
2.4.1. Flow Control	20
2.4.2. Influence on Aerodynamic Performance	21
2.4.3. Noise Control	22
2.5. Parametric Designs of the Present Models	28
2.5.1. Design Based on Skin Friction.....	29
2.5.2. Design Based on Aperture Parameters.....	31
2.5.3. Design Based on Flow Characteristics.....	32
2.5.4. Design Based on Sawtooth Parameters.....	32
2.5.5. Future Studies	33
2.6. Numerical Analysis	34
2.7. Summary.....	39
CHAPTER THREE: METHODOLOGY.....	40
3.1. Introduction.....	40
3.2. Model Descriptions.....	41

3.2.1. Baseline Model	42
3.2.2. Serrated Trailing-Edge Configuration	43
3.2.3. Combed Trailing-Edge Type	45
3.2.4. Comb-Serrated Trailing-Edge Model	46
3.2.5. Poro-Serrated Trailing-Edge Configuration.....	47
3.3. Numerical Method	48
3.3.1. Computational Domain and Boundary Conditions.....	49
3.3.2. Spatial Grid	51
3.3.3. Numerical Scheme	53
3.3.4. Data Validation	60
3.4. Experimental Set-Up	61
3.4.1. Flow Facility	61
3.4.2. Particle Image Velocimetry (PIV)	63
3.4.3. Surface Reflection.....	65
3.5. Summary.....	67
CHAPTER FOUR: AERODYNAMIC AND FLOW FIELD INVESTIGATIONS.....	68
4.1. Introduction.....	68
4.2. Computational Simulation	69
4.2.1. Two-Dimensional Numerical Simulation	69
4.2.1.1 Comparison with other Study	69
4.2.1.2 Mean Aerodynamic Characteristics.....	71
4.2.2. Three-Dimensional Numerical Simulation	78
4.2.2.1 Validation of the Computational Method.....	79
4.2.2.2 Baseline Flow Field	82
4.2.2.3 Modified Trailing-Edge Flow Field	85
4.2.3. Summary of the Numerical Simulation	92
4.3. Experimental Results	93
4.3.1. Streamwise Velocity Field	93
4.3.2. Flow Velocity Distribution	98
4.3.3. Spanwise Vorticity	105
4.3.4. Summary of the Experimental Work	112
4.4. Summary.....	113
CHAPTER FIVE: AEROACOUSTIC SIMULATIONS.....	114
5.1. Introduction.....	114
5.2. Comparison with other Study	114
5.3. Far-Field Noise Prediction.....	116
5.3.1. Surface Pressure Fluctuations	116
5.3.2. Sound Pressure Level.....	121
5.3.3. Peak Noise Level	126
5.3.4. Peak Frequency	130
5.3.5. Directivity Pattern	134
5.4. Summary.....	136
CHAPTER SIX: CONCLUSION AND RECOMMENDATIONS	138
6.1. Objective 1 – Conclusion 1	138
6.2. Objective 2 – Conclusion 2	139

6.3. Objective 3 – Conclusion 3	140
6.4. Objective 4 – Conclusion 4	141
6.5. Recommendations for Further Studies	141
REFERENCES.....	143
PUBLICATIONS	155
APPENDIX A: ISO-POINTS JOURNAL	156
APPENDIX B: ISO-SURFACE JOURNAL	159
APPENDIX C: AUTOMATIC JOURNAL	163



LIST OF TABLES

Table 2.1	Comparison of previous trailing edge designs, limitations, and proposed present study design	36
Table 2.2	Comparison of previous trailing edge designs, limitations, and proposed present study design	40
Table 3.1	Parameters Used in 2D Particle Image Velocimetry (PIV) Measurements	67



LIST OF FIGURES

Figure 1.1	An Example of Noise Spectra of An Airfoil Discrete Tonal Noise (Arcondoulis, Arcondoulis, Doolan, & Zander, 2005)	2
Figure 1.2	The Unique Feather Features of the Owl, Key to its Silent Flight	4
Figure 2.1	Effect of Angle of attack on Separation Bubble	14
Figure 2.2	Types of Airfoil Self-Noise (Thomas F Brooks Et Al., 1989)	16
Figure 2.3	Necessary Criterion for Whistle Noise Emission (Desquesnes Et Al., 2007)	19
Figure 2.4	Sketch of a serrated trailing-edge incorporating the investigated dimensions of h and λ (Gruber et al., 2011a)	24
Figure 2.5	Relationship between Skin Friction Ratio and Reynolds Number Based on Aperture Diameter	31
Figure 2.6	Relationship between Skin Friction Ratio and Depth-to-Diameter Ratio (Hwang, 2004)	32
Figure 2.7	Relationship between Skin Friction Ratio against void fraction (Hwang, 2004)	33
Figure 3.1	Flowchart of the methodology	43
Figure 3.2	Side view of the airfoil inside test section	44
Figure 3.3	Geometry of NACA0015 Airfoil Used in this Research	45
Figure 3.4	Top View of the Baseline Airfoil Model	45
Figure 3.5	Top View of the Serrated Model	46
Figure 3.6	Top View of the Serrated Model	46
Figure 3.7	Top View of the Comb Configuration	47
Figure 3.8	Top View of the Comb Configuration	47
Figure 3.9	Top View of the Comb-Serrated Model	48
Figure 3.10	Top View of the Comb Serrated Configuration	49
Figure 3.11	Top View of the Poro-Serrated Model	50
Figure 3.12	Top View of the Poro-Serrated Configuration	50
Figure 3.13	Boundaries and Dimensions of 2D Analysis Domain	52

Figure 3.14	Boundaries and Dimensions of 3D Analysis Domain	52
Figure 3.15	(a) C-Type Grid Topology (b) Detailed View of the LE (c) Detailed View of the TE	53
Figure 3.16	(a) Mesh Convergence Analysis at $Re = 8.4 \times 10^4$ (b) Mesh Convergence Analysis at $Re = 1.7 \times 10^5$	54
Figure 3.17	Detailed View of the Mesh Around the Airfoil and at the TE	55
Figure 3.18	Schematic diagram illustrating the receiver locations	62
Figure 3.19	Turbulence Intensity as a Function of the Vertical Distance (UPNM, 2022)	64
Figure 3.20	Schematic of UPNM Open Loop Wind Tunnel (UPNM, 2014)	64
Figure 3.21	Schematic of PIV Setup in the Wind Tunnel	65
Figure 3.22	Surface Reflection from Musou and Flat Black Painted Surface at $\alpha = 0^0$	69
Figure 4.1	Comparison of Cl at Different Reynolds Numbers	72
Figure 4.2	Comparison of Cd at Different Reynolds Numbers	72
Figure 4.3	Pressure Coefficient at Different Reynolds Numbers	75
Figure 4.4	Skin Friction Coefficient at Different Reynolds Numbers	75
Figure 4.5	Mean Streamlines at Different Reynolds Numbers	77
Figure 4.6	Movement of Laminar Separation Bubble on the Suction of NACA 0015	78
Figure 4.7	Movement of Laminar Separation Bubble Pressure Side	78
Figure 4.8	Average Velocity Profile on the Pressure Side	79
Figure 4.9	Average Velocity Profile on the Suction Side	79
Figure 4.10	Comparison of the Present Work with a Numerical Study.	81
Figure 4.11	Validation of the Predicted Values with the Experimental Data	82
Figure 4.12	Validation of Numerical Result (a) with the Experimental Work (b) at $\alpha = 0^0$	83
Figure 4.13	Validation of Numerical Result (a) with the Experimental Work (b) at $\alpha = 0^0$	84
Figure 4.14	Pressure and Skin Friction Coefficient of the Baseline Airfoil at $\alpha = 0^0$	85
Figure 4.15	X-Velocity Magnitude of the Baseline Airfoil at $\alpha = 0^0$	86
Figure 4.16	Velocity Profile of the Baseline Airfoil at $\alpha = 0^0$	87

Figure 4.17	Pressure Coefficient of the Modified Models at $\alpha = 0^0$	89
Figure 4.18	Skin Friction Coefficient of the Modified Models at $\alpha = 0^0$	89
Figure 4.19	X-Velocity Contour at the Tip of the Modified Models ($\alpha = 0^0$).	91
Figure 4.20	X-Velocity Contour at the Root of the Modified Models ($\alpha = 0^0$)	92
Figure 4.21	Top View Contour of X-Velocity Component for the Modified Models ($\alpha = 0^0$)	93
Figure 4.22	Velocity Profile of the Modified Airfoil Models at $\alpha = 0^0$	94
Figure 4.23	Streamwise Velocity Component at $\alpha = 0^0$	96
Figure 4.24	Streamwise Velocity Component at $\alpha = 2^0$	97
Figure 4.25	Streamwise Velocity Component at $\alpha = 3^0$	98
Figure 4.26	Streamwise Velocity Component at $\alpha = 6^0$	98
Figure 4.27	Streamwise Velocity Component at $\alpha = 8^0$	100
Figure 4.28	Streamwise Velocity Component at $\alpha = 10^0$	101
Figure 4.29	Velocity Profile at $\alpha = 0^0$	102
Figure 4.30	Velocity Profile at $\alpha = 2^0$	103
Figure 4.31	Velocity Profile at $\alpha = 3^0$	104
Figure 4.32	Velocity Profile at $\alpha = 6^0$	105
Figure 4.33	Velocity Profile at $\alpha = 8^0$	106
Figure 4.34	Velocity Profile at $\alpha = 10^0$	107
Figure 4.35	Spanwise Vorticity at $\alpha = 0^0$	109
Figure 4.36	Spanwise Vorticity at $\alpha = 2^0$	109
Figure 4.37	Spanwise Vorticity at $\alpha = 3^0$	111
Figure 4.38	Spanwise Vorticity at $\alpha = 6^0$	112
Figure 4.39	Spanwise Vorticity at $\alpha = 8^0$	114
Figure 4.40	Spanwise Vorticity at $\alpha = 10^0$	114
Figure 5.1	Normalized Surface Pressure Fluctuations at $\alpha = 4^0$	119
Figure 5.2	Time Histories Of The Normalized Wall Pressure at $\alpha = 0^0$	120
Figure 5.3	Time Histories Of The Normalized Wall Pressure at $\alpha = 1^0$	122
Figure 5.4	Time Histories Of The Normalized Wall Pressure at $\alpha = -1^0$	122
Figure 5.5	Time Histories Of The Normalized Wall Pressure at $\alpha = 2^0$	123
Figure 5.6	Time Histories Of The Normalized Wall Pressure at $\alpha = -2^0$	125

Figure 5.7	Sound Pressure Level as a Function of Frequency at the Suction Side (a) $\alpha = 0^{\circ}$ (b) $\alpha = 1^{\circ}$ (c) $\alpha = -1^{\circ}$ (d) $\alpha = 2^{\circ}$ And (e) $\alpha = -2^{\circ}$	126
Figure 5.8	Sound Pressure Level as a Function of Frequency at the Wake Region (a) $\alpha = 0^{\circ}$ (b) $\alpha = 1^{\circ}$ (c) $\alpha = -1^{\circ}$ (d) $\alpha = 2^{\circ}$ And (e) $\alpha = -2^{\circ}$	128
Figure 5.9	Sound Pressure Level as a Function of Frequency at the Pressure Side (a) $\alpha = 0^{\circ}$ (b) $\alpha = 1^{\circ}$ (c) $\alpha = -1^{\circ}$ (d) $\alpha = 2^{\circ}$ And (e) $\alpha = -2^{\circ}$	129
Figure 5.10	The Influence of Angle of attack on the Maximum Noise Level on the Suction Side of the Airfoil	131
Figure 5.11	The Influence of Angle of attack on the Maximum Noise Level at the Wake Region of the Airfoil	132
Figure 5.12	The Influence of Angle of attack on Maximum Noise Level on the Pressure Side of the Airfoil	133
Figure 5.13	The Frequency of the Highest Noise Level on the Suction Side for Various Angles of Attack	135
Figure 5.14	The Frequency of the Highest Noise Level at the Wake Region for Various Angles of Attack	136
Figure 5.15	The Frequency of the Highest Noise Level on the Pressure Side for Various Angles of Attack	138
Figure 5.16	The Directivity of the Acoustic Signals Measured at a Radial Distance of 12 Chords from the Airfoil Center	140

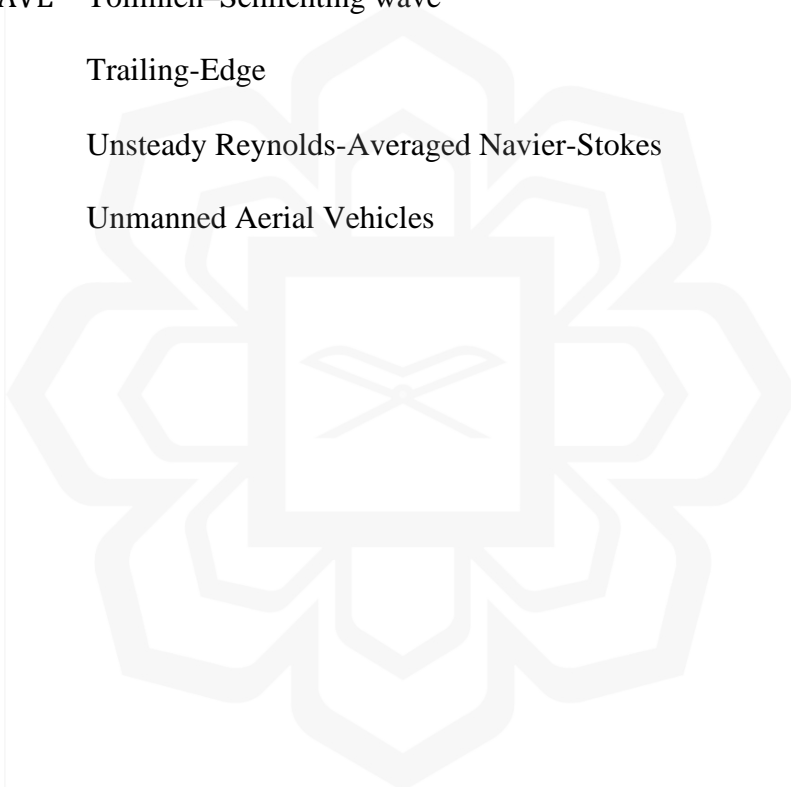
LIST OF SYMBOLS

c	Chord Length
C_d	Drag Coefficient
C_f	Skin Friction Coefficient
C_l	Lift Coefficient
C_p	Pressure Coefficient
E	Porosity
f_n	Centre frequency of the broadband noise
f_s	Series of Secondary Tone
$2h$	Height of the sawtooth part
l	Extent of the porous region
P'	Normalized Pressure Fluctuation
Δt	Interval Time
U	Free-Stream Velocity
V	Normal Velocity
ω_z	Spanwise Vorticity
Δx	Displacement
α	Angle of attack
α_s	Angle of ridges with respect to the flow direction
λ	Wavelength of the ridges

LIST OF ABBREVIATIONS

2D	Two-Dimensional
3D	Three-Dimensional
AOA	Angle of attack
BL	Boundary Layer
CAA	Computational Aeroacoustics
Cd	Drag Coefficient
CFD	Computational Fluid Dynamic
Cl	Lift Coefficient
DNS	Direct Numerical Simulation
dB	Decibels
FW – H	Ffowcs Williams–Hawkings
HLFC	Hybrid Laminar Flow Control
LBL	Laminar Boundary Layer
LE	Leading-Edge
LES	Large Eddy Simulation
LFC	Laminar Flow Control
LSB	Laminar Separation Bubble
MAVs	Micro Air Vehicles
MBT	Micro-Blowing Technology
NLF	Natural Laminar Flow
PTU	Programmable Timing Unit
PIV	Particle Image Velocimetry

RANS	Reynolds-Averaged Navier-Stokes
Re	Reynolds Number
SA	Spalart-Allmaras Turbulence Model
SGS	Subgrid-Scale
SPL	Sound Pressure Level
SPL _{1/3}	Third Octave Sound Pressure Level
SST	Shear-Stress Transport
TS – WAVE	Tollmien–Schlichting wave
TE	Trailing-Edge
URANS	Unsteady Reynolds-Averaged Navier-Stokes
UAVs	Unmanned Aerial Vehicles



CHAPTER ONE

INTRODUCTION

1.1. OVERVIEW

The introduction chapter of this thesis includes a complete review of the study background, problem statement, research philosophy, scope, limitations, and objectives. This chapter commences with an overview of the introduction to the topic under consideration, followed by a concise description of the research problem and the reasoning for the suggested solution based on the philosophical approach of the study. The scope of the research is clearly defined, with a special focus on addressing the problem statement. The research objectives are then provided in a systematic and ordered way, offering a roadmap for the completion of the study. Finally, the chapter concludes with the outline of the thesis, offering a comprehensive summary of the organization and content of the research.

1.2. BACKGROUND OF THE STUDY

Noise pollution is a continuous issue that substantially influences the environment and the well-being of humans. Loud and undesired noises can induce disruption and stress and might be regarded as a severe environmental stressor. Research has found that airfoils operating within low to moderate Reynolds numbers ($Re = 10^4 - 10^5$) are known to emit a unique sort of noise known as whistle-like tonal noise. This form of noise adds to the total environmental noise and is viewed as discomforting by people exposed to it (Wagner et al., 2007). Tonal noise may be experienced in several of circumstances, such as on blunt models and airfoil-like designs, buildings, fans, wind turbines, unmanned aerial vehicles (UAVs), and more. Given the widespread prevalence and effect of tone noise, it is vital to know the underlying mechanisms and situations that create it. This information may be utilized to design effective methods for limiting its impact and decreasing the related environmental and health hazards. Furthermore, understanding the behaviour of tonal noise can lead to the development of

new technology and ways to decrease noise pollution, increase human quality of life, and safeguard the environment.

Schumacher et al. (2014) first described the generation of discrete tonal noise from airfoil surfaces operating at relatively moderate Reynolds numbers (Schumacher et al. 2014). The tonal noise is a composition of broadband noise focused on a single frequency, and discrete tonal noise. The occurrence of tonal noise is influenced by the thickness of the Trailing-edge (TE) and the Boundary Layer (BL) displacement thickness, as evidenced by Ramirez and Wolf (Ramírez & Wolf, 2016). The noise generation can also be affected by various geometric factors, such as thickness, chord, profile, and Angle of attack. Other factors such as spanwise curvature and surface roughness also play a role but are subject to strict engineering constraints. Paterson et al. (1973) reported the presence of discrete and numerous tones in a ladder-like structural pattern, which is dependent on the frequency and free-stream velocity. Tonal noise with high intensity is often regarded as more disturbing than broadband noise. Arbey & Bataille (1983) ascribed the broadband contribution to the diffraction of pressure waves near the TE. The discrete frequencies are made of a primary frequency tone with the maximum intensity, and its respective secondary frequency tones are uniformly spaced, as indicated in Figure 1.1.

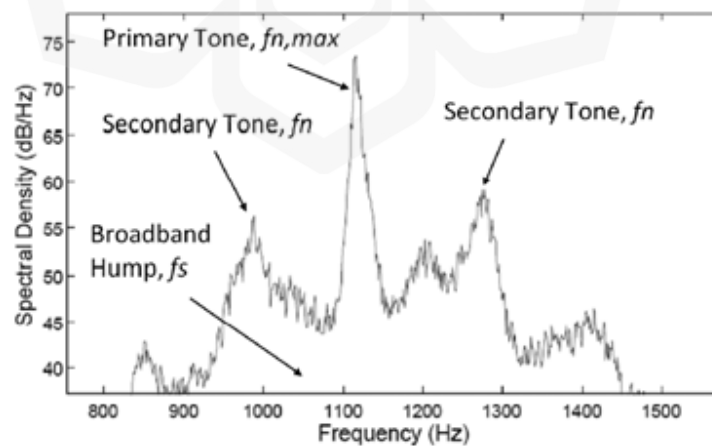


Figure 1.1 An example of noise spectra of an airfoil discrete tonal noise (Arcondoulis et al., 2005)

The aviation industry has made tremendous progress in lowering the noise created by aircraft airfoils and helicopter blades via acoustically adapted materials and design improvements. Efforts to regulate fluid flow have led to the suggestion of strategies such as Laminar Flow Control (LFC), Natural Laminar Flow (NLF), and Hybrid Laminar Flow Control (HLFC) (Joslin, 1998). However, the practical implementation of NLF is hindered by its association with substantial pressure drag. Milestones have been made in the knowledge of flow physics, acoustic wave scattering, and noise propagation, leading to the introduction of various trailing-edge noise-reducing technologies (Joslin, 1998). These techniques are categorized into passive and active control approaches, with the former aiming to improve scattering conditions by altering physical and geometrical features of the TE and the latter acting on changing the flow structure through unsteady pressure fluctuations upstream of the trailing edge. Recently, numerous passive control approaches have been proposed and investigated, including using serrations, porous materials, finlets, surface treatments, shape optimization, morphing, and flexible materials. These strategies seek to increase aerodynamic performance while minimizing noise produced at the TE (Tze et al., 2016).

The study of silent flight in birds, notably the owl, has been a topic of continuous research in of aerodynamics. Figure 1.2 highlights the distinctive feather characteristics of the owl, which play a significant role in decreasing noise and contributing to the owl's reputation as the quietest flying bird. This has prompted contemporary research attempts to study the processes behind the owl's ability to fly so softly and to apply these results to numerous sectors, such as aviation. The attention to the owl's feather characteristics underlines the value of learning from nature and transferring these lessons into human technology. By acquiring a greater knowledge of the owl's quiet flight, researchers want to create more effective and efficient noise reduction solutions for many applications. This study primarily focuses on applying poro-serrated, serrated, combed, and comb-serrated trailing-edge designs to optimize the flow structure and minimize noise generation at the TE, as shown in Figure 3.4 – 3.12.

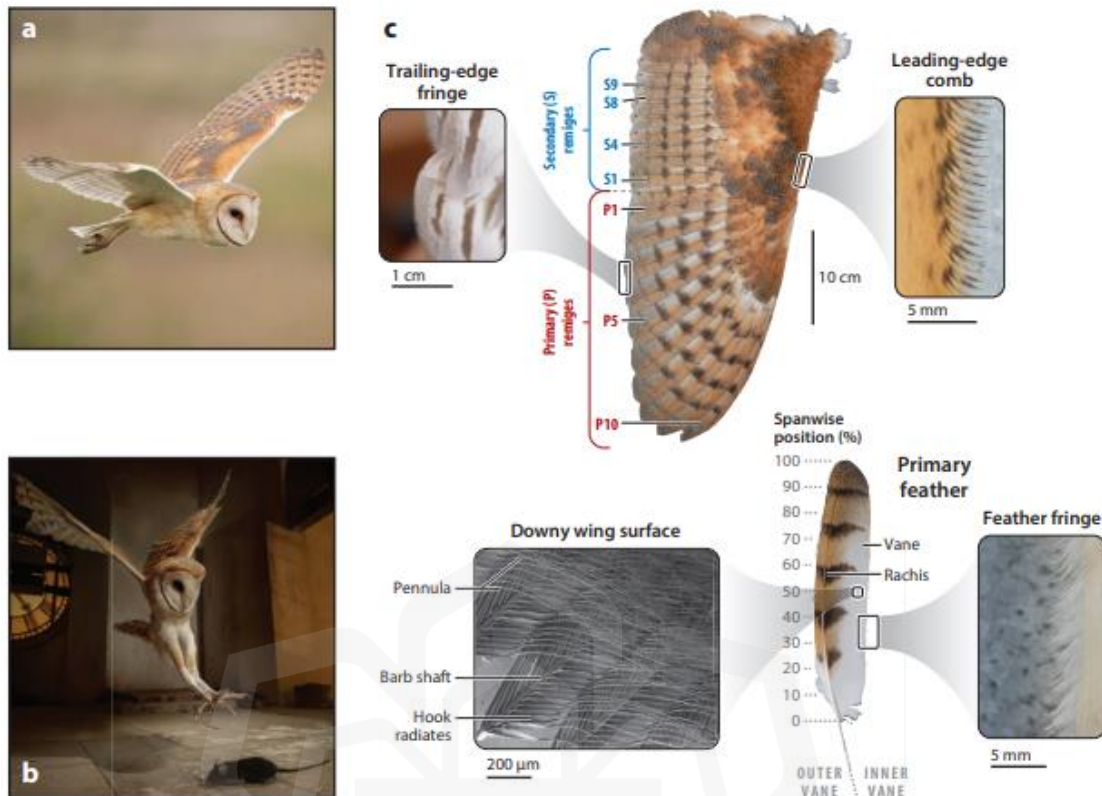


Figure 1.2 The Unique Feather Features of the Owl, Key to Its Silent Flight (Jaworski & Peake, 2020).

1.3. STATEMENT OF THE PROBLEM

Aircraft noise has become a critical concern since the 1970s as the number of airports and commercial aircraft has increased. The adverse effects of aeroplane noise on human health have necessitated stricter regulations in the aviation sector. Although great progress has been achieved in decreasing jet engine noise, experts have advocated for more investigations into reducing noise from other aircraft elements. Various experimental, computational, and theoretical studies have focused on minimizing trailing-edge noise, with serrations being regarded as one of the most successful methods based on bio-inspired research. However, the efficiency of serrations, comb, and porous trailing edge is still not well understood. It is reliant on flow topology, and most experiments have been undertaken at low Reynolds numbers ($R_e \approx 10^4$). Furthermore, the collective impact of the serrated and comb design models has not been

thoroughly examined. Upon closer examination of owl feathers, it is evident that their shapes exhibit inconsistency. Consequently, it is imperative to delve comprehensively into this aspect to grasp its contribution to effective noise reduction. This is precisely why the comb-serrated model is being employed as one of the models in this study.

Additionally, there is a need to broaden the current understanding of the discrete tonal behaviour of NACA0015 airfoil, as relatively little experimental and numerical analysis has been undertaken at moderate Reynolds numbers and various angles of attack, which have more practical applications. Additionally, the NACA 0015 airfoil is preferred due to its utilization as a symmetric airfoil with increased thickness in compared to the more frequently employed NACA 0012 airfoil. Investigating the effect of this difference in thickness becomes essential in comprehending the distinctive tonal behavior exhibited by the NACA 0015 airfoil. The airfoil tonal emission is tied to the amplification of naturally existing instabilities inside the laminar boundary layer (LBL); however, these instabilities alone do not always contribute to tonal noise. Instead, the extent and location of the LSB also have an impact on the emitted tonal noise. Despite the viability of this finding, the fundamental physical reasons causing airfoil tonal noise still need to be fully understood.

The present research strives to thoroughly understand the tonal noise process and related physical phenomena by conducting wind tunnel tests and CFD simulations, evaluating the flow structure and tonal noise over an airfoil impacted by whistle tonal noise. Additionally, the study will evaluate the influence of passive flow control systems on airfoil noise emission and flow structure. Given the limited research on controlling airfoil tonal noise without negatively affecting flow structure, the study seeks to find effective methods to improve the noise performance and enhance the flow characteristics at relatively moderate Reynolds number (1.7×10^5) and varying angles of attack ($-2 \leq \alpha \leq 2$ deg). The selection of Reynolds numbers and angles of attack for investigation is based on the observation that discrete tonal noise becomes more noticeable at lower Reynolds numbers and angles of attack, following previous research findings.

1.4. RESEARCH PHILOSOPHY

The scientific concept driving the analysis of airfoil tonal noise and its reduction is based on the knowledge of the link between the physics of flow and the generation of tonal noise. This research will tackle this problem by conducting flow visualization using wind tunnel experiments and CFD simulations to examine the flow structure and tonal noise mechanism over an airfoil under the effect of whistle tonal noise. It has been noted that the induced tonal radiation is dependent primarily on the Reynolds number and Angle of attack. Therefore, this research will examine the airfoil tonal emission at moderate Reynolds numbers and varied angles of attack that have more practical uses. In addition, the influence of flow control techniques on airfoil noise emission and flow structure needs to be explored. Therefore, this research will also attempt to conduct passive flow control over the NACA0015 airfoil to enhance its noise performance and flow characteristics. Overall, this study is motivated by the notion that a better understanding of the underlying physics of flow and tonal noise will lead to developing effective and efficient noise-reducing strategies for many practical applications.

1.5. RESEARCH OBJECTIVES

The main objectives of this research are:

- 1- To determine the influence of Reynolds number and angles of attack on the flow field structure over NACA0015 airfoil.
- 2- To investigate the noise emitted over NACA0015 airfoil at different angles of attack and a moderate Reynolds number.
- 3- To determine the effect of flow control techniques on the aerodynamic and flow field characteristics.
- 4- To evaluate effective noise-reducing methods for airfoil tonal noise based on passive techniques.

1.6. RESEARCH SCOPE

The study focuses on examining the link between the physics of flow and the generation of tonal noise over a NACA0015 airfoil as relatively little experimental and numerical